

Influence of hypoxia on retinal progenitor and ganglion cells in human induced pluripotent stem cell-derived retinal organoids

Jin-Lin Du^{1,2}, Li-Xiong Gao³, Tao Wang¹, Zi Ye², Hong-Yu Li^{1,2}, Wen Li^{1,2}, Quan Zeng⁴, Jia-Fei Xi⁴, Wen Yue⁴, Zhao-Hui Li^{1,2}

¹Medical School of Chinese PLA, Beijing 100853, China

²Senior Department of Ophthalmology, the Third Medical Center of Chinese PLA General Hospital, Beijing 100039, China

³Department of Ophthalmology, the 6th Medical Center of PLA General Hospital, Beijing 100048, China

⁴Stem Cell and Regenerative Medicine Lab, Beijing Institute of Radiation Medicine, Beijing 100850, China

Correspondence to: Zhao-Hui Li. Senior Department of Ophthalmology, the Third Medical Center of Chinese PLA General Hospital, Beijing 100039, China. zhaohuili650@hotmail.com. Wen Yue and Jia-Fei Xi. Stem Cell and Regenerative Medicine Lab, Beijing Institute of Radiation Medicine, No.27 Taiping Road, Haidian District, Beijing 100850, China. yuewen0206@126.com; xi_jiafei@126.com

Received: 2023-02-03 Accepted: 2023-08-03

Abstract

• **AIM:** To observe the effect of low oxygen concentration on the neural retina in human induced pluripotent stem cell (hiPSC)-derived retinal organoids (ROs).

• **METHODS:** The hiPSC and a three-dimensional culture method were used for the experiments. Generated embryoid bodies (EBs) were randomly and equally divided into hypoxic and normoxic groups. Photographs of the EBs were taken on days 38, 45, and 52, and the corresponding volume of EBs was calculated. Simultaneously, samples were collected at these three timepoints, followed by fixation, sectioning, and immunofluorescence.

• **RESULTS:** The proportion of Ki67-positive proliferating cells increased steadily on day 38; this proliferation-promoting effect tended to increase tissue density rather than tissue volume. On days 45 and 52, the two groups had relatively similar ratios of Ki67-positive cells. Further immunofluorescence analysis showed that the ratio of SOX2-positive cells significantly increased within the neural retina on day 52 ($P < 0.05$). In contrast, the percentage of PAX6- and CHX10-positive cells significantly decreased

following hypoxia treatment at all three timepoints ($P < 0.01$), except for CHX10 at day 45 ($P > 0.05$). Moreover, the proportion of PAX6/TUJ1⁺ cells within the neural retinas increased considerably ($P < 0.01$, < 0.05 , < 0.05 respectively).

• **CONCLUSION:** Low oxygen promotes stemness and proliferation of neural retinas, suggesting that hypoxic conditions can enlarge the retinal progenitor cell pool in hiPSC-derived ROs.

• **KEYWORDS:** hypoxia; retinal organoid; retinal progenitor cells; retinal ganglion cells

DOI:10.18240/ijo.2023.10.03

Citation: Du JL, Gao LX, Wang T, Ye Z, Li HY, Li W, Zeng Q, Xi JF, Yue W, Li ZH. Influence of hypoxia on retinal progenitor and ganglion cells in human induced pluripotent stem cell-derived retinal organoids. *Int J Ophthalmol* 2023;16(10):1574-1581

INTRODUCTION

A low-oxygen environment naturally benefits cell proliferation and morphogenesis during early placental development in the first trimester. In later pregnancy, an increased oxygen concentration is required for protein synthesis, supporting the rapid growth of the fetus^[1]. This is closely coordinated with the regulation of oxygen levels, which underlies the development of various organogenic processes in the body. This low-oxygen environment during embryonic development *in vivo* is known as physiological hypoxia. The oxygen concentration ranges from 1%–5% (8–38 mm Hg PO₂) in this physiological hypoxic microenvironment, which is less than the adult arterial oxygen pressure (10%–13.15% oxygen equivalent to 75–100 mm Hg PO₂)^[2]. This physiological hypoxia is typically considered protective, as antioxidants are not expressed until approximately 8–9wk of gestation^[3–4]. Hypoxia is a critical element that is responsible for regulating embryogenesis and stem cell differentiation in the early stages of embryonic development^[5]. Studies have shown that hypoxia is essential for restricting human embryonic stem cell (hESC) differentiation and maintaining stemness^[6]. Hypoxia can also

facilitate vascular differentiation of human pluripotent stem cell (hPSC), including hESC and human induced pluripotent stem cell (hiPSC)^[6-8].

Currently, the effect of hypoxia on human retinal development remains largely unknown. However, ethical barriers remain in the way of further collecting direct evidence of the influence of hypoxia on human retinal development. The emergence of a three-dimensional (3D) culture of hPSC has expanded our research tools, allowing us to generate more predictable models in an organoid 3D configuration, generating micro-physiologically active systems in a dish and serving as the first selection for drug trials and personalized medicine^[9-12]. Recently, hPSC-derived retinal organoids (ROs) have been used to discover the pathological mechanisms underlying retinal diseases, test new drugs, and study retinal development^[13-16]. Based on this technology, our previous study confirmed the influence of intermittent high oxygen levels on retinal development^[17]. The results showed that hyperoxia significantly improved the growth of ROs and further influenced the apical-basal characteristics of ROs.

In this study, by using serum-free floating culture of embryoid body-like aggregates with quick aggregation (SFEBq) and hypoxia treatment, the effects of low oxygen concentration on the growth of neural retina tissue were investigated. The influence of hypoxia on retinal progenitor cells (RPCs) and as well as mature retinal neurons was also discovered.

MATERIALS AND METHODS

Ethical Approval All research that involved human cells and tissues was carried out in accordance with the principles of the Helsinki Declaration.

hiPSC Culture and Generation of hiPSC-Derived Retinal Organoids As previously shown, the hiPSC line (FMCPGHi001-A) used in this study was validated using standardised methods^[18]. The hiPSC line was grown in mTeSR1 media (StemCell Technologies, Vancouver, Canada) on Matrigel-coated (Corning Inc., Corning, NY, USA) plates and passaged at 80% confluence every 5–7d. Cultures were regularly tested and maintained free of mycoplasma. 3D induction was done using the SFEBq method, but with a few adjustments^[19-20]. hiPSC was dissociated into single cells for 3min at 37°C in Accutase containing 20 mol/L Y-27632 (StemCell Technologies). After centrifugation (200 g for 5min) and resuspension, 1.2×10^4 single hiPSC was reaggreated in a 96-well V-bottomed conical plate (PrimeSurface; Sumitomo Bakelite, Tokyo, Japan) with 100 μ L growth factor-free chemically defined medium (gfCDM) supplemented with 10% knockout serum replacement (KSR; Gibco, Thermo Fisher Scientific, Waltham, MA, USA), 45% Iscove's modified Dulbecco's medium-GlutaMAX (Gibco, USA), 45% Ham's F12-GlutaMAX (Gibco), 1% chemically defined

lipid concentrate (Gibco), monothioglycerol (450 mmol/L; Sigma-Aldrich, Germany), and 20 μ mol/L Y-27632 (StemCell Technologies). The day of the hiPSC plated was considered day 0. On day 6, 1.5 nmol/L (55 ng/mL) recombinant human bone morphogenetic protein 4 (rhBMP4; R&D Systems, Minneapolis, MN, USA) was added to the culture medium. rhBMP4 was diluted by half on days 9, 12, and 15. On day 18, embryoid bodies (EBs) were transferred into a low-adhesion 6-well plate containing neural retina (NR) differentiation medium, which contained the DMEM/F12-Glutamax medium (Gibco), 1% N2 supplement (Gibco), 10% foetal bovine serum (FBS; Gibco), 0.5 mmol/L retinoic acid (Sigma-Aldrich), and 0.1 mmol/L taurine (Sigma-Aldrich). The culture medium was changed every three days until day 30.

Hypoxia Treatment On day 30, all EBs were randomly and equally divided into two groups. EBs in normoxic group were cultivated at 37°C in a humidified atmosphere containing 5% CO₂ and 20% O₂, whereas EBs in hypoxic group were cultivated in an atmosphere containing 5% CO₂ and 5% O₂. Both incubators were produced by Thermo Fisher Scientific. Nitrogen was continuously supplied to a low-oxygen incubator to maintain a hypoxic environment. The culture medium was changed every three days, and the EBs remained in a low oxygen environment.

Measurement of the Volume of Embryoid Bodies On days 38, 45, and 52 in the normoxic and hypoxic groups, three EBs were selected randomly and photographed at 100 \times magnification using a digital camera (DS-Ri2; Nikon, Tokyo, Japan). Bright-field images were obtained using a light microscope (Ti S, Nikon). For better resolution, individual pictures of the same EB were stitched and converted into an entire image using Adobe Photoshop CC (version 20.0.2; Adobe Systems, San Jose, CA, USA) for further analysis. The volume of the EBs formed were calculated based on our previous study^[17]. In summary, there were two basic shapes: 1) an ellipsoid with one short axis (a) and one vertical long axis (b), and 2) a collection of spherical segments (n : the number of protuberances) with a base radius (r_n) and a top height (h_n ; Figure 1G). The EBs volume is calculated as follows:

$$V_{RO} = V_0 + \sum_{n=0,1,2,3,\dots} V_n$$

where V_0 represents the volume of the ellipsoid, and V_n represents the volume of the spherical segments. The importance of an RO is as follows:

$$V_{RO} = \frac{4}{3} \pi a b^2 + \sum_{n=0,1,2,3,\dots} \frac{\pi h_n}{6} (3r_n^2 + h_n^2)$$

Fixation, Section, and Immunofluorescence Analysis of Retinal Organoids On days 38, 45, and 52, three ROs

were randomly selected from the normoxic and hypoxic groups ($n=9$). Paraffin embedding of ROs were performed as previously described^[17]. After washing in 0.01 mol/L PBS, the ROs were fixed in 4% paraformaldehyde for 12h. ROs were embedded in paraffin wax after being dehydrated with a graded series of ethanol and xylene. Then, 5- μm thick paraffin slices were obtained using a paraffin microtome (Leica, Wetzlar, Germany). The extracts were dried at 37°C for two days before being stored at room temperature (RT). Before performing immunofluorescence analysis, three areas across the central part of the RO were selected under a microscope. After deparaffinisation and rehydration in xylene and ethanol, immunohistochemistry was performed as previously described^[17]. In brief, after being treated with 0.2% Triton X-100 (RT, 30min) and 10% donkey serum (RT, 30min), sections were incubated with the following primary antibodies: anti-Ki67 (1:200; Abcam, Cambridge, UK), anti-PAX6 (1:200; Abcam), anti-SOX2 (1:200; Abcam), anti- β tubulin III (1:200; Beyotime, Shanghai, China), anti-CHX10 (1:200; Santa Cruz Technologies, USA), anti-BRN3 (1:100; Santa Cruz Technologies) and anti-NESTIN (1:200; Sigma-Aldrich) in 10% donkey serum (overnight, 4°C). The next day, after washing in 0.01 mol/L PBS, Alexa Fluor 488- or 568-conjugated secondary antibodies were added (1:400; RT, 1h). The sections were counterstained with DAPI (1:500, Sigma-Aldrich) before being scanned using a laser scanning microscope (Axio Imager Z2; Carl Zeiss, Jena, Germany).

Cell Counting and Statistical Analysis Three comparable sections across the centre of the ROs were selected and stained in the normoxic and hypoxic groups at days 38, 45, and 52. Cell numbers were counted using Image J software (NIH, Bethesda, MD, USA). After photos were captured, three 200 \times 200 μm^2 ectangular regions were selected at random from each segment. The number of immunofluorescence-positive and DAPI-stained cells in the room was counted manually. The cell density of ROs was calculated by manually counting the number of DAPI-stained cells per unit area. More specifically, as the location of SOX2- and CHX10-positive cells was restricted to the outer layer of ROs, the ratio of these two markers was calculated within this layer. Similarly, as the location of PAX6- and BRN3-positive cells was limited to the inner layer of the ROs, the percentage of PAX6- and BRN3-positive cells was calculated within this layer. For TUJ1-positive cell counting, three 100 \times 100 μm^2 rectangular areas were randomly chosen at the inner layer of the ROs. The number of TUJ1-positive cells was manually counted. In sections double-stained with TUJ1 and PAX6, TUJ1-positive cells within 200 \times 200 μm^2 rectangular areas were counted manually. In those TUJ1 positive cells, PAX6-positive and -negative cells were also estimated. For statistical analysis, the

cellular data were analysed using SPSS software V22.0 (IBM, Armonk, USA). Significance analysis was performed using the group *t*-test. All data are expressed as mean \pm standard error. The significance level was set at $P<0.05$.

RESULTS

hiPSC Identification and Retinal Organoids Generation

Using feeder-free culture methods, hiPSC exhibited a classical round clone shape. A cell counting kit-8 (CCK-8) proliferation assay of hiPSC showed an exponential increase, and immunofluorescence showed that hiPSC expressed stemness markers including NANOG, OCT4, and SOX2. We further tested the pluripotency of hiPSC using a teratoma formation assay. With haematoxylin and eosin staining, teratomas were found to be generated from hiPSC. These results showed that hiPSC exhibits all the characteristics of hPSC. By using the SFEBq culture method, we found that hiPSC forms round EBs. The SFEBq culture was performed on day 0; on day 6, rhBMP4 was added to the culture system at a final concentration of 1.5 nmol/L. After sequential half-dilution of rhBMP4, EBs gradually formed ROs. On day 30, over 90% of the ROs formed irregular oval shapes with a continuous semi-transparent epithelium. ROs were randomly divided into the hypoxic group that received 5% O₂ hypoxia treatment on day 30 and a normoxic group that was continuously cultured under a typical oxygen environment.

Influence of Hypoxia on the Proliferation of Retinal Organoids

To examine the proliferation-promoting effect, images of ROs under a light microscope were taken on days 38, 45, and 52. The ROs generated were calculated based on our previous study^[17]. The results showed that the volume of ROs gradually increased in hypoxic and normoxic environments. However, the volume of ROs under hypoxic treatment was significantly decreased compared to that under normoxic treatment (Figure 1A–1H). We also noticed that the transparency of neuroepithelia for hypoxic groups was poorer than that for normoxic groups (Figure 1A–1F), indicating a relatively higher density in hypoxic group. By counting the cell number within same visual fields and calculating cell density, we proved that the cell density in the hypoxic groups was significantly higher than that for normoxic groups (all $P<0.05$; Figure 1I). To further examine the proliferation-influencing effect, Ki67 immunofluorescence analysis was performed. Our results showed that Ki67-positive cells were mainly located in the outer layer of NR (Figure 2A–2F). The ratio of Ki67-positive cells within the ROs increased significantly after 5% hypoxic treatment compared to that in the normoxic group on day 38 ($P<0.05$; Figure 2A–2B, 2G). This significant proliferation-promoting effect continued until two and three weeks later. On days 45 and 52, the ratio of Ki67-positive cells within the ROs was still higher in the hypoxic group than in

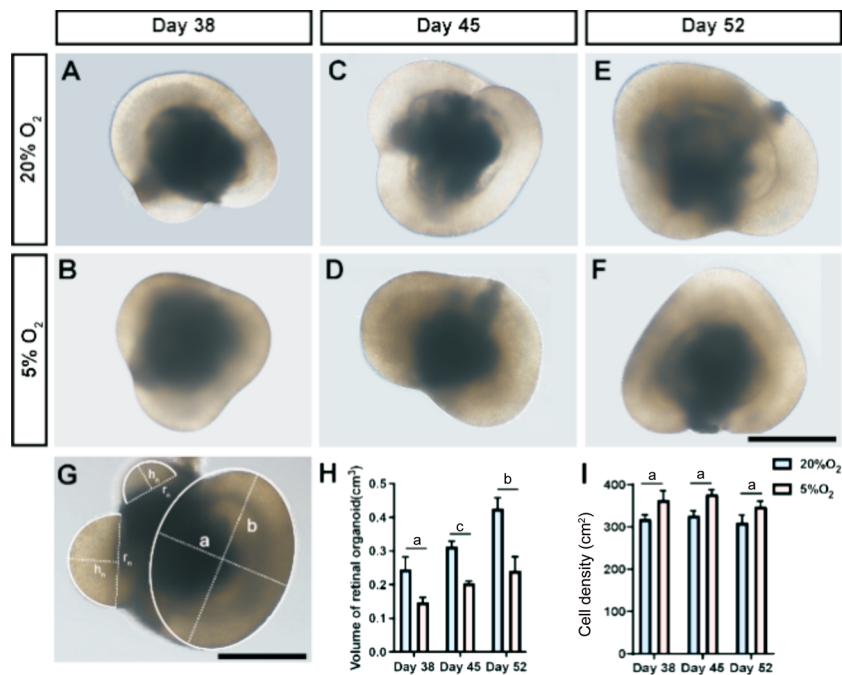


Figure 1 The volume of ROs growing under hypoxic treatment was significantly lower than in normoxic treatment A–F: Optical microscope images of ROs in day 38, 20% O₂ (A), day 38, 5% O₂ (B), day 45, 20% O₂ (C), day 45, 5% O₂ (D), day 52, 20% O₂ (E), and day 52, 5% O₂ (F). G: Schematic diagram measuring the volume of the ROs. Scale bar: 500 μm. They are divided into two basic shapes: an ellipsoid with one short axis (a) and one vertical long axis (b), and the remaining spheres (n) are considered to have a base radius (r_n) and a top height (h_n). H: Statistical diagram of the volume of ROs. I: Statistical diagram of the cell density within ROs. The volume of ROs growing under hypoxic treatment was significantly lower than that under normoxic treatment (^a*P*<0.05, ^b*P*<0.01, ^c*P*<0.001). ROs: Retinal organoids.

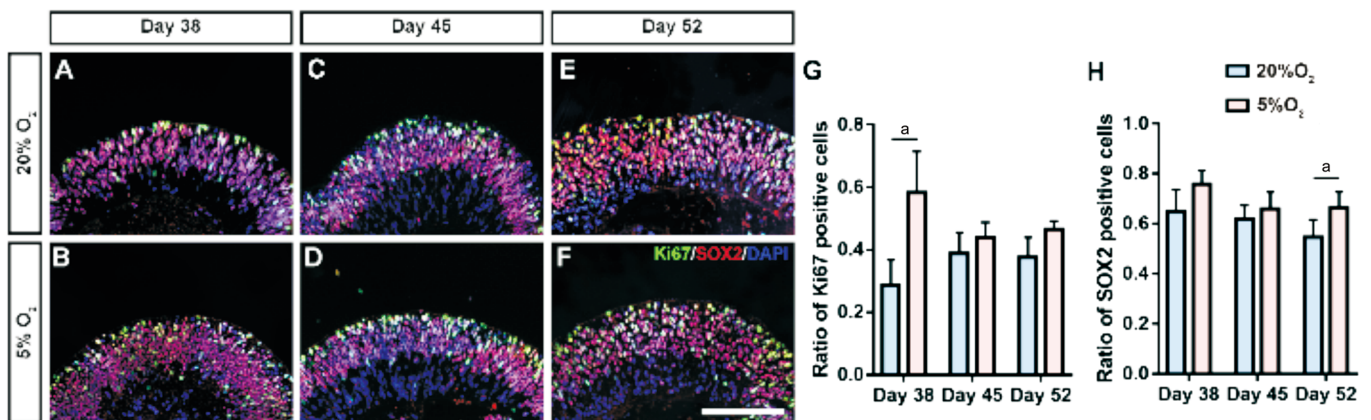


Figure 2 The effects of hypoxia on the proliferation of NRs and the expression of SOX2-positive cells A–F: Ki67-immunoreactive proliferating cells (green) of NRs and expression of SOX2-positive cells (red) in day 38, 20% O₂ (A), day 38, 5% O₂ (B), day 45, 20% O₂ (C), day 45, 5% O₂ (D), day 52, 20% O₂ (E), and day 52, 5% O₂ (F). Scale bar: 50 μm. G: Statistical analysis of the Ki67-immunoreactive proliferating cell ratio of NRs in two groups at three timepoints, respectively. H: Statistical analysis of the ratio of SOX2-positive cells in two groups (^a*P*<0.05). NRs: Neural retinas.

the normoxic group, although the difference was not significant (*P*>0.05; Figure 2C–2G). These results indicated that hypoxic promotes cell proliferation during early NR development in ROs. This effect tends to influence the proliferation state of retinal cells rather than the volume of general ROs.

Influence of Hypoxic Treatment on Retinal Progenitor Cells CHX10, SOX2, and PAX6 staining was performed to examine the effect of hypoxia on early retinogenesis. The results showed that CHX10- and SOX2-positive cells were mainly located in the outer layer of ROs, while PAX6-positive

cells were primarily located in the inner layer of ROs (Figures 2A–2F, 3A–3F). Statistical analysis showed that the ratio of SOX2-positive cells between the hypoxic and normoxic groups increased on days 38, 45, and 52 (Figure 2A–2F, 2H). However, this difference was only significant on day 52 (*P*<0.05; Figure 2E, 2F, 2H). CHX10 and PAX6 showed different results. Specifically, the ratio of these two markers showed a decreasing trend following hypoxic treatment (Figure 3A–3F). Statistical analysis showed that on days 38, 45, and 52, the ratio of PAX6-positive cells within the ROs decreased

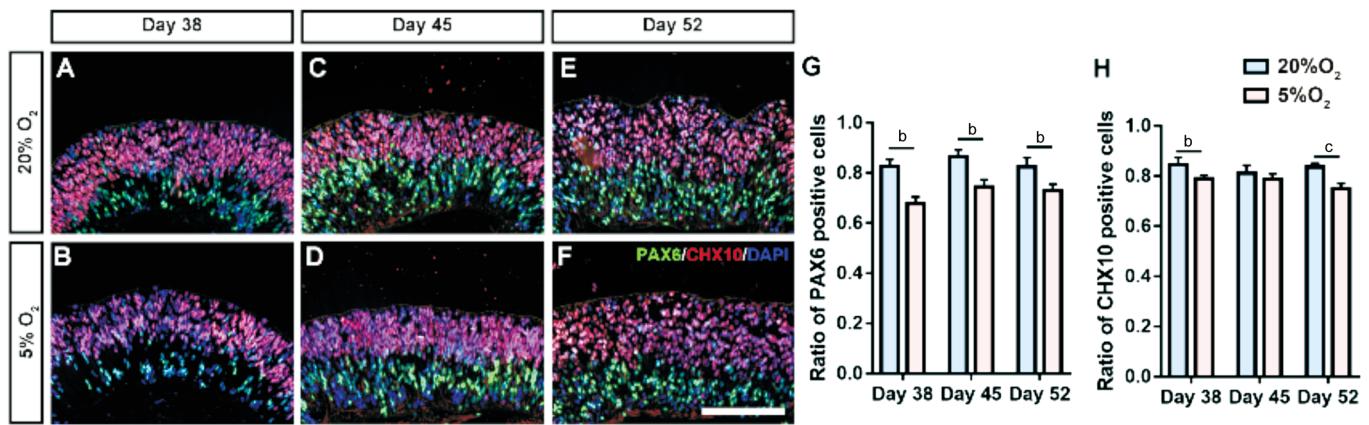


Figure 3 The effects of hypoxic treatment on the expression of PAX6- and CHX10-positive cells A–F: PAX6 (green) and CHX10 (red) double-staining of NRs in day 38, 20% O₂ (A); day 38, 5% O₂ (B); day 45, 20% O₂ (C); day 45, 5% O₂ (D); day 52, 20% O₂ (E); and day 52, 5% O₂ (F). Scale bar: 50 μ m. G: Statistical analysis of the ratio of PAX6-positive cells within retinal organoids in two groups at three timepoints, respectively. H: Statistical analysis of the CHX10-positive cell ratio in two groups at three timepoints (^b $P < 0.01$, ^c $P < 0.001$). NRs: Neural retinas.

significantly after 5% hypoxia treatment compared to that in the normoxic group (all $P < 0.01$; Figure 3A–3G). The ratio of CHX10-positive cells also decreased significantly after 5% hypoxia treatment compared with that in the normoxic group on days 38 and 52 ($P < 0.01$ and < 0.001 , respectively; Figure 3A, 3B, 3E, 3F, 3H). On day 45, the ratio of CHX10-positive cells within the ROs decreased after 5% hypoxia treatment, without significance ($P > 0.05$; Figure 3C, 3D, 3H). In addition, it is worth noting that when focusing on the ratio of PAX6-positive cells, the difference between hypoxic and normoxic groups continued to shrink as time progressed (Figure 3A–3F, 3G).

Influence of Hypoxia on the Differentiation of TUJ1-Positive Cells To further determine the influence of hypoxia on cell differentiation, a TUJ1 immunofluorescence assay was performed. TUJ1 was used to mark differentiated retinal ganglion cells (RGCs) in our previous work. To better represent the migration of TUJ1-positive cells, NESTIN was counterstained with TUJ1. Usually, in ROs, cells proliferate at the apical side, and the generated RGCs migrate along the scaffold formed by NESTIN-positive retinal stem cells to the basal side. Our results showed no significant difference in the ratio of migrating TUJ1-positive cells between the hypoxic and normoxic groups on days 38, 45, and 52 (all $P > 0.05$; Figure 4A–4F, 4G). To illustrate that TUJ1 positive cells are RGCs, the immunofluorescence of BRN3 was also performed. Similarly, results of BRN3 fluorescence staining showed no statistical difference between these two groups ($P > 0.05$). To further examine the differentiation state of TUJ1-positive cells, double staining of TUJ1 and PAX6 was performed. The results showed that the ratio of PAX6-positive cells within TUJ1-positive cells decreased significantly following hypoxic treatment on days 38, 45, and 52 ($P < 0.01$, < 0.01 , < 0.05 , respectively; Figure 5A–5F, 5G), whereas the ratio of PAX6-negative cells within TUJ1-positive cells increased

significantly following hypoxic treatment on days 38, 45, and 52 ($P < 0.01$, < 0.05 , < 0.05 ; respectively; Figure 5A–5F, 5H). This result was due to the changing trend in PAX6-positive cells following hypoxic treatment.

DISCUSSION

In the present study, using the SFEBq 3D culture method, the influence of hypoxia on the development of human ROs was investigated. Hypoxia significantly promoted retinal cell proliferation during the early developmental stage (before 40d). Hypoxic treatment at a later stage had no effect on cell proliferation. In addition, the expansion-promoting effects of hypoxia increased the cell density of ROs rather than increasing the volume. We also found that the impact of hypoxia tends to restrict the progenitor status to a less-differentiated condition, as reflected by more embryonic marker-positive cells and fewer RPC marker-positive cells^[7]. We found that hypoxia could influence human retinal development, filling gaps our previous high-oxygen study did not find. With intermittent high-oxygen treatment and SFEBq culture, our previous study showed that the volume of ROs significantly increased after hyperoxic treatment. The formation of PAX6-positive cells and the maturation of RGCs were also enhanced^[17]. Unlike high oxygen levels, hypoxia only has a proliferation-promoting effect at the early developmental stage. In addition, it tends to increase the density of the ROs rather than their volume. Moreover, the ratio of PAX6- and CHX10-positive RPCs significantly decreased following hypoxic treatment, which is in the opposite direction to high-oxygen treatment^[21–22].

Our results confirmed that the proliferation-promoting effect of hypoxia is confined to the early retinal developmental stage. This could be a consequence of the stemness-maintaining effects of hypoxia. Recent studies have shown that hypoxia can stimulate the proliferation of dermal papilla

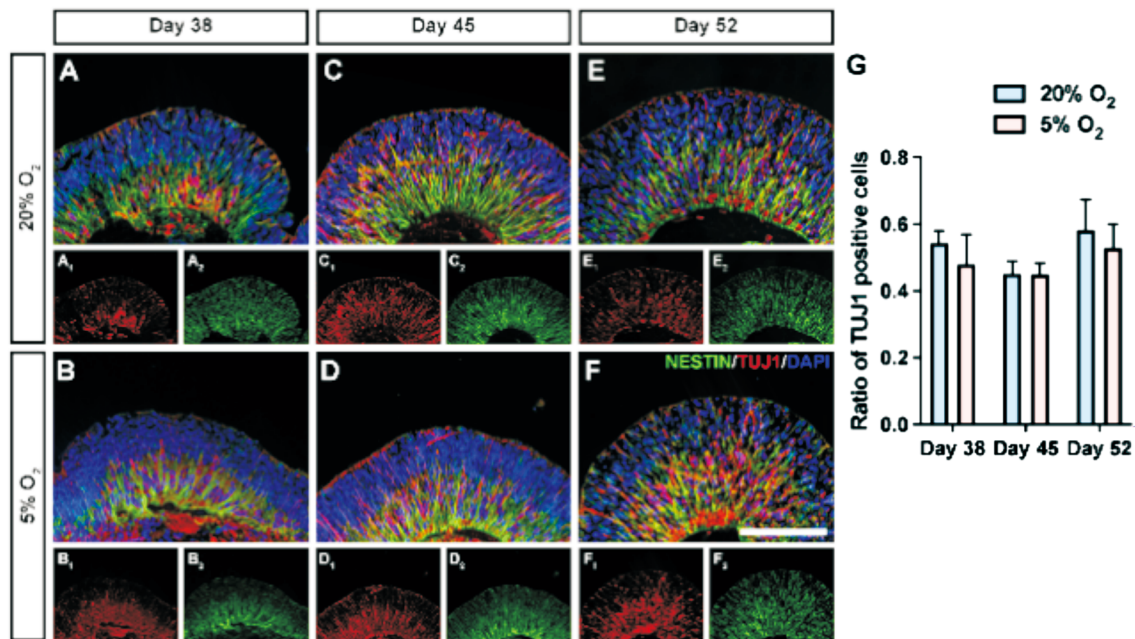


Figure 4 The effects of hypoxia on the expression of TUJ1- and NESTIN-positive cells A–F: TUJ1 (red) and NESTIN (green) double-staining of NRs in day 38, 20% O₂ (A); day 38, 5% O₂ (B); day 45, 20% O₂ (C); day 45, 5% O₂ (D); day 52, 20% O₂ (E); and day 52, 5% O₂ (F). Scale bar: 50 μm. G: Statistical analysis of the ratio of TUJ1-positive cells within retinal organoids in two groups at three timepoints, respectively. NRs: Neural retinas.

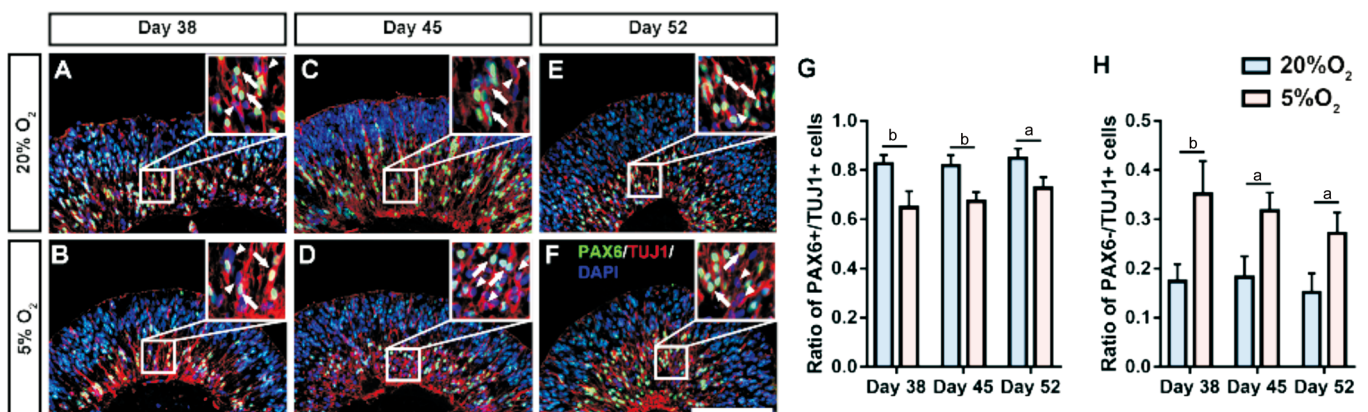


Figure 5 To further examine the differentiation state of TUJ1-positive cells, double staining of TUJ1 and PAX6 was performed A–F: TUJ1 (red) and PAX6 (green) double-staining of NRs in day 38, 20% O₂ (A); day 38, 5% O₂ (B); day 45, 20% O₂ (C); day 45, 5% O₂ (D); day 52, 20% O₂ (E); and day 52, 5% O₂ (F). Scale bars: 50 μm. G: Statistical analysis of PAX6-positive cells within TUJ1-positive cells and the ratio of NRs in two groups at three timepoints, respectively. H: Statistical analysis of PAX6-negative cells within the TUJ1-positive cell ratio in two groups at three timepoints, respectively (^a*P*<0.05, ^b*P*<0.01). NRs: Neural retinas.

cells^[23], dental pulp stem cells^[24], neural stem cells^[25], and mesenchymal stem cells^[26], among others^[27-29]. To some extent, dermal papilla cells can be considered a unique source of mesenchymal stem cells^[30]. As shown through these other stem cell studies, hypoxia mainly promotes the proliferation of stem cells. Usually, high oxygen tension tends to induce the differentiation of stem cells, whereas low oxygen tension tends to maintain stemness. This could be a consequence of redox homeostasis^[31]. Under hypoxia, the intracellular reactive oxygen species level decreases significantly, which further increases hypoxia-inducible factor (HIF) expression, reduces p38 expression levels, and promotes the self-renewal

of stem cells^[32-33]. This mechanism better illustrates our findings. As there are more undifferentiated stem cells in the early developmental stage, hypoxia mainly promotes the proliferation of these naïve stem cells during this period. In general, stem cells have smaller volumes than differentiated cells do. As this self-renewal process significantly enlarges stem cell pools, the proliferation-promoting effect of hypoxia could increase tissue density rather than tissue volume. Specifically, our results showed that hypoxia decreased the PAX6- and CHX10-positive RPCs ratio^[22-34]. A previous study using the adherent differentiation method to generate RPCs showed that a low-oxygen environment could increase

the percentage of RPCs co-expressing PAX6 and CHX10^[35]. This contradicts our results. However, the difference in the differentiation models could be the reason for this. On the one hand, for adherent culture, differentiation of PSC occurred more quickly; the PAX6- and CHX10-positive RPCs are the stem cell pool in the adherent differentiation method. In contrast, our 3D differentiation protocol generated naturally differentiated NRs from EBs. Under these circumstances, SOX2 and other ESC act as a higher-grade stem cell pool, while PAX6- or CHX10-positive RPCs are relatively more differentiated cells^[36-37]. In addition, hypoxia can significantly induce the expression of SOX2 *via* HIF-1 α and HIF-2 α signalling molecules^[38]. These results are all based on the notion that hypoxia promotes stemness and the proliferation of stem cells^[4,7]. Our previous study confirmed that TUJ1-positive cells within ROs were BRN3-positive RGCs^[17,39-40]. A recent single-cell sequencing study showed that iPSC-derived RGCs can be divided into subtypes^[41-42]. PAX6-positive or -negative subtypes could be distinguished from the whole sample. Although no significant difference was found in the ratio of TUJ1-positive cells, the percentage of PAX6⁺/TUJ1⁺ cells significantly increased after hypoxia exposure. In contrast, the proportion of PAX6⁺/TUJ1⁺ cells significantly decreased. This result indicates that the formation of a subgroup of PAX6-positive RGCs was prohibited. Our previous study confirmed that the generation, migration, and maturation of RGCs were enhanced following high-oxygen treatment^[17,43]. Thus, the development of RGCs was partially inhibited after low-oxygen treatment. There are several limitations of the current study. First, we only provided morphological results illustrating the influence of hypoxia. The mechanism was not explored. Second, the observation period was only 2wk after hypoxia exposure. Long-term influence of hypoxia is needed to be discovered. Third, to low oxygen treatment could be optimised to better reflect the actual foetal development, rather than constant 5% O₂ in the current study.

In the present study, the influence of hypoxia on human retinal development was investigated using the SFEBq culture method. Our results confirmed the stemness/proliferation-promoting effects of hypoxia. More specifically, this effect tends to increase tissue density rather than volume. Further immunofluorescence analysis showed that the ratio of SOX2-positive cells increased, whereas the percentage of PAX6- and CHX10-positive cells decreased following hypoxia treatment. Moreover, the proportion of PAX6⁺/TUJ1⁺ cells within ROs significantly increased. These results provide primary evidence for the influence of periodic hypoxia on human retinal development, which may help future retinal developmental studies better understand physiological hypoxia's effects during embryonic development.

ACKNOWLEDGEMENTS

Authors' contributions: Du JL and Gao LX: conceptualization, methodology, software, investigation, formal analysis, writing-original draft. Wang T and Ye Z: resources. Li HY and Li W: visualization, investigation. Zeng Q: supervision. Xi JF, Yue W and Li ZH: conceptualization, funding acquisition, resources, supervision, writing-review & editing.

Foundations: Supported by the National Nature Science Foundation of China (No.82070937; No.81870640; No.82000923).

Conflicts of Interest: Du JL, None; Gao LX, None; Wang T, None; Ye Z, None; Li HY, None; Li W, None; Zeng Q, None; Xi JF, None; Yue W, None; Li ZH, None.

REFERENCES

- Burton GJ. Oxygen, the Janus gas; its effects on human placental development and function. *J Anat* 2009;215(1):27-35.
- Fathollahipour S, Patil PS, Leipzig ND. Oxygen regulation in development: lessons from embryogenesis towards tissue engineering. *Cells Tissues Organs* 2019;205(5-6):350-371.
- Watson AL, Palmer ME, Jauniaux E, Burton GJ. Variations in expression of copper/zinc superoxide dismutase in villous trophoblast of the human placenta with gestational age. *Placenta* 1997;18(4):295-299.
- Grimm C, Willmann G. Hypoxia in the eye: a two-sided coin. *High Alt Med Biol* 2012;13(3):169-175.
- Hawkins KE, Sharp TV, McKay TR. The role of hypoxia in stem cell potency and differentiation. *Regen Med* 2013;8(6):771-782.
- Podkalicka P, Stepniewski J, Mucha O, Kachamakova-Trojanowska N, Dulak J, Łoboda A. Hypoxia as a driving force of pluripotent stem cell reprogramming and differentiation to endothelial cells. *Biomolecules* 2020;10(12):1614.
- Mohyeldin A, Garzón-Muvdi T, Quiñones-Hinojosa A. Oxygen in stem cell biology: a critical component of the stem cell niche. *Cell Stem Cell* 2010;7(2):150-161.
- Ezashi T, Das P, Roberts RM. Low O₂ tensions and the prevention of differentiation of hES cells. *Proc Natl Acad Sci U S A* 2005;102(13):4783-4788.
- Eiraku M, Takata N, Ishibashi H, *et al.* Self-organizing optic-cup morphogenesis in three-dimensional culture. *Nature* 2011;472(7341):51-56.
- Ravi M, Paramesh V, Kaviya SR, Anuradha E, Solomon FD. 3D cell culture systems: advantages and applications. *J Cell Physiol* 2015;230(1):16-26.
- Langhans SA. Three-dimensional *in vitro* cell culture models in drug discovery and drug repositioning. *Front Pharmacol* 2018;9:6.
- Whelan KA, Muir AB, Nakagawa H. Esophageal 3D culture systems as modeling tools in esophageal epithelial pathobiology and personalized medicine. *Cell Mol Gastroenterol Hepatol* 2018;5(4):461-478.
- O'Hara-Wright M, Gonzalez-Cordero A. Retinal organoids: a window into human retinal development. *Development* 2020;147(24):dev189746.

- 14 Norrie JL, Nityanandam A, Lai KR, *et al.* Retinoblastoma from human stem cell-derived retinal organoids. *Nat Commun* 2021;12(1):4535.
- 15 Aasen DM, Vergara MN. New drug discovery paradigms for retinal diseases: a focus on retinal organoids. *J Ocular Pharmacol Ther* 2020;36(1):18-24.
- 16 Reinhard J, Joachim SC, Faissner A. Extracellular matrix remodeling during retinal development. *Exp Eye Res* 2015;133:132-140.
- 17 Gao LX, Chen X, Zeng YX, *et al.* Intermittent high oxygen influences the formation of neural retinal tissue from human embryonic stem cells. *Sci Rep* 2016;6:29944.
- 18 Wang T, Tang W, Zeng Q, *et al.* Generation of induced pluripotent stem cell line (FMCPGHi001-A) from a 25-year-old Chinese Han healthy male donor. *Stem Cell Res* 2022;60:102735.
- 19 Kuwahara A, Ozone C, Nakano T, Saito K, Eiraku M, Sasai Y. Generation of a ciliary margin-like stem cell niche from self-organizing human retinal tissue. *Nat Commun* 2015;6:6286.
- 20 Zou T, Gao LX, Zeng YX, *et al.* Organoid-derived C-Kit+/SSEA4-human retinal progenitor cells promote a protective retinal microenvironment during transplantation in rodents. *Nat Commun* 2019;10:1205.
- 21 Rowan S, Cepko CL. A POU factor binding site upstream of the Chx10 homeobox gene is required for Chx10 expression in subsets of retinal progenitor cells and bipolar cells. *Dev Biol* 2005;281(2):240-255.
- 22 Belecky-Adams T, Tomarev S, Li HS, Ploder L, McInnes RR, Sundin O, Adler R. Pax-6, Prox 1, and Chx10 homeobox gene expression correlates with phenotypic fate of retinal precursor cells. *Invest Ophthalmol Vis Sci* 1997;38(7):1293-1303.
- 23 Ye J, Tang XL, Long YZ, Chu Z, Zhou Q, Lin BJ. The effect of hypoxia on the proliferation capacity of dermal papilla cell by regulating lactate dehydrogenase. *J Cosmet Dermatol* 2021;20(2):684-690.
- 24 Yang AD, Wang LL, Jiang K, Lei L, Li HX. Nuclear receptor coactivator 4-mediated ferritinophagy drives proliferation of dental pulp stem cells in hypoxia. *Biochem Biophys Res Commun* 2021;554:123-130.
- 25 Li GF, Guan YY, Gu YK, Guo MY, Ma W, Shao QQ, Liu J, Ji XM. Intermittent hypoxic conditioning restores neurological dysfunction of mice induced by long-term hypoxia. *CNS Neurosci Ther* 2023;29(1):202-215.
- 26 Feng XD, Zhu JQ, Zhou JH, *et al.* Hypoxia-inducible factor-1 α -mediated upregulation of CD99 promotes the proliferation of placental mesenchymal stem cells by regulating ERK1/2. *World J Stem Cells* 2021;13(4):317-330.
- 27 Wang J, Wu H, Peng YX, Zhao Y, Qin YY, Zhang YB, Xiao ZB. Hypoxia adipose stem cell-derived exosomes promote high-quality healing of diabetic wound involves activation of PI3K/Akt pathways. *J Nanobiotechnology* 2021;19(1):202.
- 28 Cao WD, Zhou Q, Wang *et al.* Hypoxia promotes glioma stem cell proliferation by enhancing the 14-3-3 β expression via the PI3K pathway. *J Immunol Res* 2022;2022:1-11.
- 29 Zhi XS, Xiong J, Wang MC, Zhang HX, Huang G, Zhao J, Zi XY, Hu YP. Physiological hypoxia enhances stemness preservation, proliferation, and bidifferentiation of induced hepatic stem cells. *Oxidative Med Cell Longev* 2018;2018:1-10.
- 30 Gan YY, Wang HL, Du LJ, *et al.* Cellular heterogeneity facilitates the functional differences between hair follicle dermal sheath cells and dermal papilla cells: a new classification system for mesenchymal cells within the hair follicle niche. *Stem Cell Rev and Rep* 2022;18(6):2016-2027.
- 31 Wang K, Zhang T, Dong Q, Nice EC, Huang CH, Wei YQ. Redox homeostasis: the linchpin in stem cell self-renewal and differentiation. *Cell Death Dis* 2013;4(3):e537.
- 32 He Y, Jian CX, Zhang HY, Zhou Y, Wu X, Zhang G, Tan YH. Hypoxia enhances periodontal ligament stem cell proliferation via the MAPK signaling pathway. *Genet Mol Res* 2016;15(4).
- 33 Tirpe AA, Gulei DA, Ciortea SM, Crivii C, Berindan-Neagoe I. Hypoxia: overview on hypoxia-mediated mechanisms with a focus on the role of HIF genes. *Int J Mol Sci* 2019;20(24):6140.
- 34 Matsushima D, Heavner W, Pevny LH. Combinatorial regulation of optic cup progenitor cell fate by SOX2 and PAX6. *Development* 2011;138(3):443-454.
- 35 Bae D, Mondragon-Teran P, Hernandez D, Ruban L, Mason C, Bhattacharya SS, Veraitch FS. Hypoxia enhances the generation of retinal progenitor cells from human induced pluripotent and embryonic stem cells. *Stem Cells Dev* 2012;21(8):1344-1355.
- 36 Bhatia B, Singhal S, Tadman DN, Khaw PT, Limb GA. SOX2 is required for adult human Müller stem cell survival and maintenance of progenicity *in vitro*. *Invest Ophthalmol Vis Sci* 2011;52(1):136.
- 37 Surzenko N, Crowl T, Bachleda A, Lee LE, Pevny L. SOX2 maintains the quiescent progenitor cell state of postnatal retinal Müller glia. *Development* 2013;140(7):1445-1456.
- 38 Bae KM, Dai Y, Vieweg J, Siemann DW. Hypoxia regulates SOX2 expression to promote prostate cancer cell invasion and sphere formation. *Am J Cancer Res* 2016;6(5):1078-1088.
- 39 Riazifar H, Jia YS, Chen J, Lynch G, Huang TS. Chemically induced specification of retinal ganglion cells from human embryonic and induced pluripotent stem cells. *Stem Cells Transl Med* 2014;3(4):424-432.
- 40 Luo ZM, Xu CC, Li KJ, *et al.* Islet1 and Brn3 expression pattern study in human retina and hiPSC-derived retinal organoid. *Stem Cells Int* 2019;2019:8786396.
- 41 Gudiseva HV, Vrathasha V, He J, Bungatavula D, O'Brien JM, Chavali VRM. Single cell sequencing of induced pluripotent stem cell derived retinal ganglion cells (iPSC-RGC) reveals distinct molecular signatures and RGC subtypes. *Genes* 2021;12(12):2015.
- 42 Fligor CM, Langer KB, Sridhar A, *et al.* Three-dimensional retinal organoids facilitate the investigation of retinal ganglion cell development, organization and neurite outgrowth from human pluripotent stem cells. *Sci Rep* 2018;8(1):14520.
- 43 Snow RL, Robson JA. Ganglion cell neurogenesis, migration and early differentiation in the chick retina. *Neuroscience* 1994;58(2):399-409.